RESEARCH PAPER | Engineering | Volume : 5 | Issue : 4 | April 2015 | ISSN - 2249-555X

A Study on a CFD Analysis of Pressure Difference on Naca0012 Airfoil by Changing Gurney Flap Height and Angle of Attack

KEYWORDS: NACA 0012 airfoil; Gurney flap; CFD analysis; Attack angle; Pressure difference; Turbulence models

Hardik S. Patel

ME (Mech-auto), Dept. of mechanical engineering, LDRP-ITR

ABSTRACT *Study of a two-dimensional CFD analysis is done to investigate the effects of angle of attack and height of gurney flap on the aerodynamic characteristics of NACA0012 airfoil. Various techniques used for plotting and modelling an airfoil is seen. Different parameters used, and its effects, in analysis like domain shape, grid cells, number of nodes in meshing, various boundary conditions is surveyed. Change in Reynolds number of fluid results in different output hence variation of lift & drag co-efficient with change in Reynolds number is analysed. Proper selection of turbulence model is an essential criterion for accurate results which shows similarity to real condition. Inappropriate model gives worthless output hence selection of most accurate turbulence model for given problem is examined. Validation of computational results with available experimental data is also observed.*

INTRODUCTION

CFD of an NACA0012 airfoil is studied over various altered parameters, resulting effects are observed and also validated with reliable experimental data which is also considered. Fully developed turbulent flow with Reynolds number (Re) is set to 6×10^6 is studies. Spallart-Allmaras, k-ε realizable, k-ω standard and k-ω Shear Stress Transport (SST) are primarily used to model viscous turbulent model. It was studied that for flow around NACA 0012 airfoil k-ω Shear Stress Transport (SST) model is the most accurate [1]. This model was proposed and developed by Menter. In the validation course the results for flow over no flapped NACA 0012 is compared with published standard data by NASA, as nearly same computational method is used to study flapped NACA 0012 airfoil. It was found that the lift coefficient was increased with a small decrease in the drag coefficient using a 1.25% chord Gurney flap. Gurney flap effectively changed the flow-field in the region of the trailing edge by introducing two contra rotating vortices aft of the flap, which altered the Kutta condition and circulation in the region. It was also noticed, however, that increasing the flap size above 2% of the wing chord length noticeably increased the drag. Gurney flap effectively increase the local camber of the trailing edge [2]. Spalart – Allmaras – one equation model, designed specifically for aerospace applications and low Reynolds number model. The simplest "complete models" of turbulence are two-equation models. The standard k- ε model falls within this class of turbulence model. Since loopholes in this models became known, two improvements made in this model: the RNG k- ε model and the realizable k- ε model. The standard k- ω model is based on the Wilcox k- ω model, which incorporates modifications for low-Reynolds-number effects, compressibility, and shear flow spreading. Variation in k- ω model is made, called SST k- ω. It is used to formulate region near wall and k- ω is used for far field. k- ε model is converted in k- ω model. SST k- ω model is refined k- ω model, is more accurate and reliable for wider class of flows [3]. In separate study the measurements were carried out for the Reynolds number of $9.7\text{x}10^4$ and $1.9\text{x}10^5$ and attack angle of 0 to 14^0 with 20 intervals to investigate the effects of these parameters on aerodynamic characteristics of NACA0012 airfoil [4]. Nonlinear relation in lift increment and gurney flap height was also noticed, where lift increased for small gurney flaps rapidly while rate was slower for big flaps. Gurney flap was analysed for six different heights ranging from 0.5% to 4% at the trailing edge perpendicular to the chord [5].

PLOTTING AND ANALYSIS

Reynolds number for the simulations is $Re=6\text{x}10^6$, the free stream temperature is 300 K, which is the same as the ambient temperature. The density of the air at the given temperature is ρ = 1.225 kg/m^3 and the viscosity is $\mu=1.7894\times10^{-5}$ kg/ms. Flow for this Reynolds number can be labelled as incompressible. This is a supposition close to reality and there is no necessity to resolve the energy equation. More number of nodes in mesh gives accurate results. Fig 1 depicts the variation of coefficient of lift with number of grid cells at stall angle of attack (16°). For greed independent solution 120000 quadrilateral cells are used in study. In this study it is assumed that inlet velocity is less turbulent that pressure outlet. Hence, for velocity inlet boundary condition turbulence intensity is considered 1% and for pressure outlet boundary5% [1].

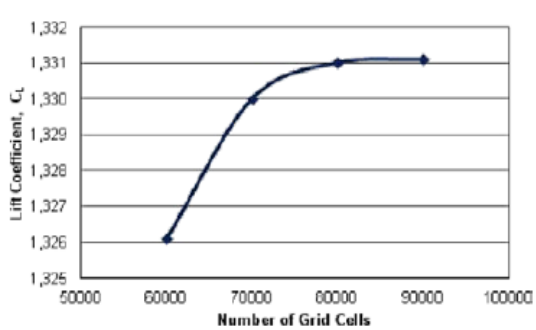

Fig 1- Graph of lift coefficient vs. number of grid cells

A different study was carried out taking Reynolds number 2.1×10^6. In this study, k-ε and Spalart-Allmaras (S-A) models were used to determine which model is successful in modelling the flow of interest. S-A model was used because of its high correlation with experimental data. The total number of grids used around 35000. Data were computed for angle of attack, α from 0° to 18° with an inter-

Volume : 5 | Issue : 4 | April 2015 | ISSN - 2249-555X

val of 2° [2]. A study was carried out for angles of attack ranging from -12 to 20 degrees. C-type grid topology with 80000 quadrilateral cells was used. For all flows, the solver solves conservation equations for mass and momentum. Additional transport equations are also solved when the flow is turbulent [3]. For gurney flaps investigation at high Reynolds number k-ε RNG model is chosen as verified by turbulence model dependency studies. Mach number is always less than 0.3, hence flow is incompressible. As it is incompressible energy equation is not used for numerical solution. The airfoil boundary is assigned as solid-wall with no-slip condition while inlet is assigned as velocity inlet and outlet is assigned as pressure-outlet conditions. Density based implicit solving scheme is used with the flow medium being air and Mach number less than 0.3. Hence the fluid is assumed to be incompressible with constant density of 1.225 kg/m^3 and dynamics viscosity of 1.7894 × 10^{-5} kg/m-s. The value of Reynolds number based on chord and inlet velocity is 2.1 × 10^6 equal to that of experimental investigations [5].

EXPERIMENTAL PROCEDURE

The blowing-type, low-speed wind tunnel which is consist of a metal duct, a honey comb, a nozzle, a straightening duct and a test section was used to measurements, as shown in Fig 2. The honey comb with a cross-sectional area of 305x305 mm^2 and the nozzle with 1.5:1 contraction ratio was used to obtain smooth streamlines and to reduce turbulent level and to prevent boundary layer separations and accelerate air flow, respectively. The tunnel has 30 m/s the maximum air velocity at the inlet of the test section with a turbulent intensity of 0.7%, run by a 5.7 kW axial blower and flow rates were adjusted by a butterfly valve within the tunnel. The static pressure measurements were carried out by using pressure tappings with a diameter of 0.5 mm and were recorded by a micro-manometer. All experiments were conducted using a wool NACA0012 airfoil with a chord length of 152 mm (C) and a span of 305 mm which was mounted in the middle of the test section of the wind tunnel, as shown in Fig 3. The flow field around the airfoil was ideally free from 3D effects due to equal span wise length with test section [4].

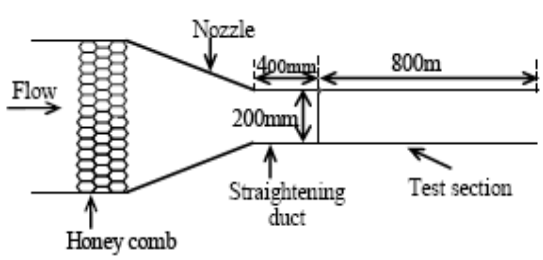

Fig 2- Schematic diagram of wind tunnel [4]

Fig 3- Experimental set up of wind tunnel [4]

RESULT AND DISCUSSION

Zero lift is observed at zero angle of attack. It is also apparent that with positive angle of attack stagnation point moves toward trailing edge on the lower surface of the airfoil as in fig 4. This pressure deviation on the upper and lower surface of the airfoil principally creates significant amount of positive lift. Different flap angle and Mach numbers (M) are studied. M>0.3 is considered as compressible. However, flow at high flap angles (δ) (i.e. 30, 40 and 50 degrees) is very unstable and it remains unconverged even after 5000 iteration in ANSYS Fluent flow solver. Hence, flow for flap angle (δ) 30, 40 and 50 degrees are slightly erratic.

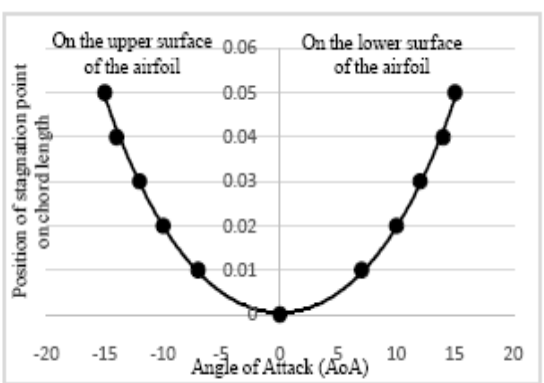

Fig 4- Variation of stagnation point with angle of attack

Results of lift coefficient changes against different Mach number with variable flap angle are shown in fig 5. Higher lift is obtained at higher deflected angles regardless of Mach number. When velocity increases i.e. up to 0.8 to 1.2 (transonic speed), lift is decreased and drag is increased. This can be dealt by thin airfoil or supercritical foil. Results of drag coefficient changes against different Mach number with variable flap angle are shown in fig 6. Drag coefficient remains somewhat constant at low Mach numbers. Sudden increase is seen when Mach number reaches up to 1[1].

Volume : 5 | Issue : 4 | April 2015 | ISSN - 2249-555X

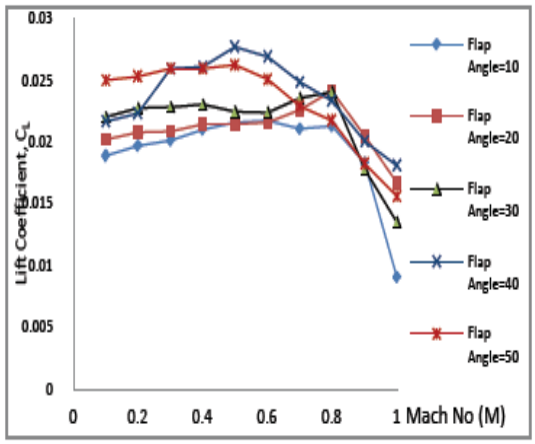

Fig 5- Lift coefficient vs. Mach number with variable flap angle

The lift co-efficient comparable with the available experimental data as in fig 7 up to α =14°. This may be due to unsteady flow behavior at higher angle of attack and particularly beyond the stall where computations assume the flow to be steady. While this is the stall angle of attack for NACA0012, in the computational result the maximum lift co-efficient occurs at α = 16°.

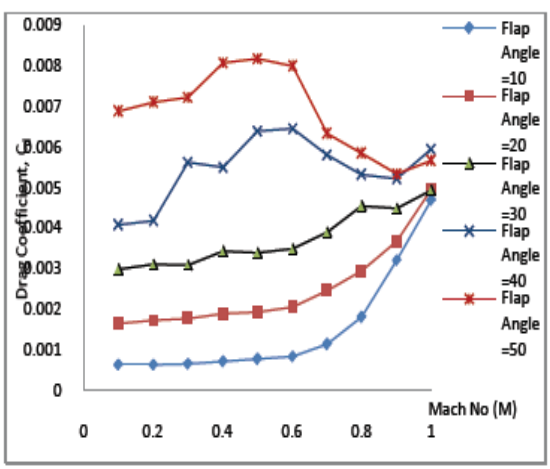

Fig 6- Drag coefficient vs. Mach number with variable flap angle

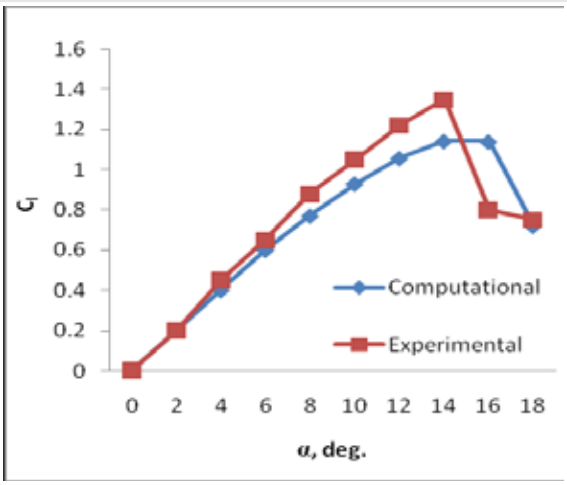

Fig 7- Lift coefficient vs. angle of attack.

The drag co-efficient also agrees well with the experimental results. The computational results show more drag than experimental results fig 8. In computational solution, the flow is fully turbulent whereas the experimental flow-field is not fully turbulent.

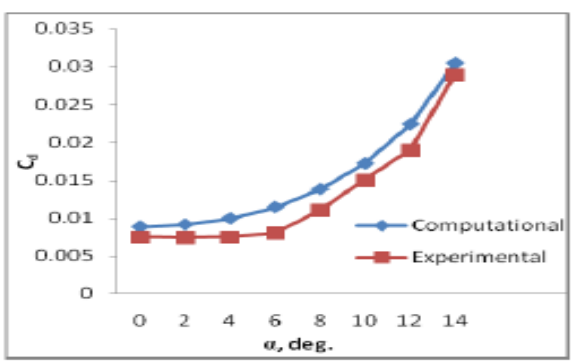

Fig 8- Drag coefficient vs. angle of attack

Under pre-stall conditions it is observed that there is good agreement of lift and drag coefficient between computational and experimental data with rectangular Gurney flap fig 9 & 10. With increase in gurney flap height C_l and C_d also increases. Fig 9 & 10 shows that for flap height 1%c C_l & C_d shows better results [2].

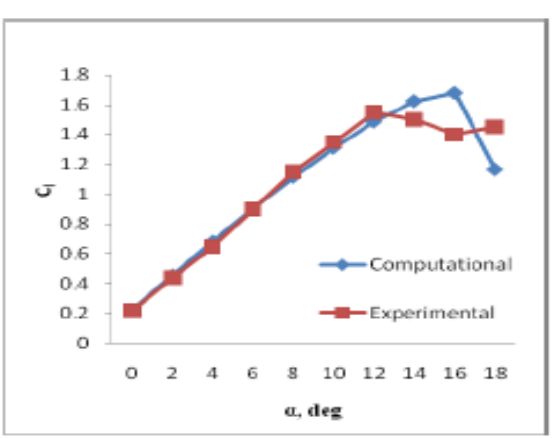

Fig 9- Coefficient of lift vs. angle of attack for airfoil with 1%c flap

Volume : 5 | Issue : 4 | April 2015 | ISSN - 2249-555X

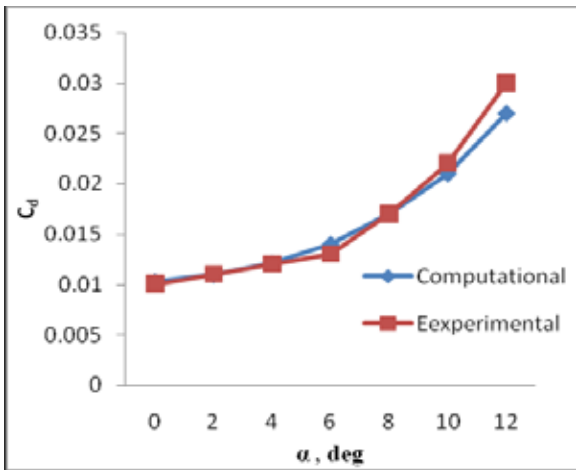

Fig 10- Coefficient of drag vs. angle of attack for airfoil with 1%c flap

At an angle of attack of roughly 15° or 16°, the flow on the upper surface of the airfoil begins to separate and a condition known as stall begins to develop fig 11. The realizable k-ε model and the SST k-w model did not have a good agreement with the experimental results. It is obvious that the Spalart - Allmaras turbulence model is the most appropriate for this simulation.

Near stall, disagreement between the data is shown. The lift coefficient peaks and the drag coefficient increases as stall increases. The predicted drag coefficients are higher than the experimental results fig 12. The trailing edge stagnation point moves slightly forward on the airfoil at low angles of attack and it jumps rapidly to leading edge at stall angle.

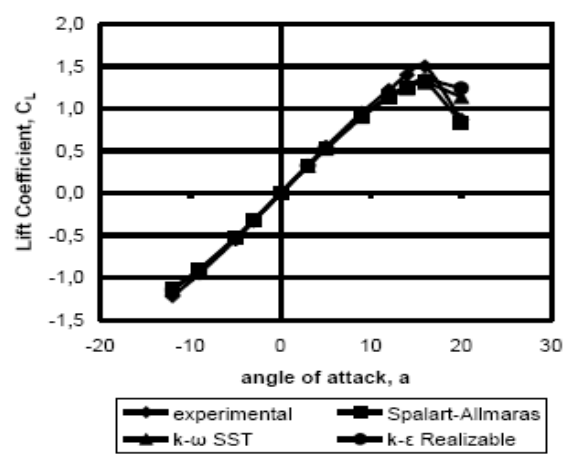

Fig 11- Comparison between experimental data and three different turbulent models simulation results of the lift coefficient curve for NACA 0012 airfoil

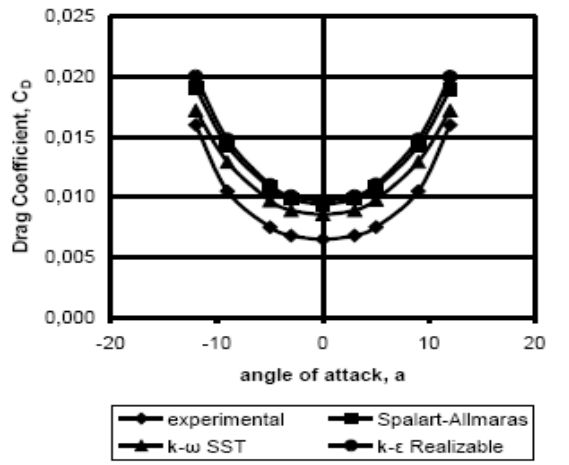

Fig 12- Comparison between experimental data and three different turbulent models simulation results of the drag coefficient curve for NACA 0012 airfoil

For all the angles of attack, the pressure coefficient had a large suction peak at the suction surface near the leading edge fig 13 & 14, and followed by a gradual increase in pressure. The stall point of the pressure side was obtained near the leading edge, where the pressure coefficient attained maximum value. Suction peaks of the suction side were in the range of -1.5 and -3.5 from the attack angle of 0^0 to 12^0 and for pressure side Cp is from -0.1 to 0.0004 for angle of attack = 0 and 12^0. Both figures shows that with increasing Reynolds number positive pressure difference decreases. Mostly affection pressure on suction side as pressure side's pressure remains as it is.

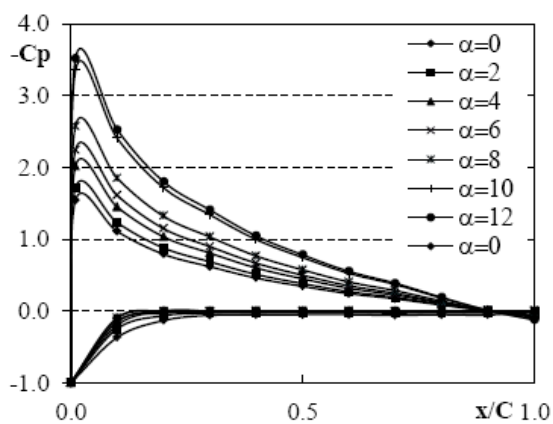

Fig 13- Pressure distributions of suction and pressure side of the airfoil at ReC=9.7x10⁴

Volume : 5 | Issue : 4 | April 2015 | ISSN - 2249-555X

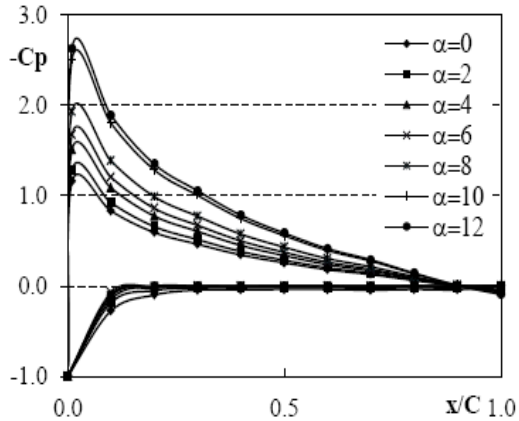

Fig 14- Pressure distributions of suction and pressure side of the airfoil at ReC=1.9x10^5

CL-AOA curve is nearly linear, The C_L increased monotonously with angle attack and reached the maximum at the angle attack of 12^0 and 13^0 at ReC=9.7x10^4 and 1.9x10^5, respectively fig 15. The occurrence of the stall at angle of attack=12^0 and 13^0 and the angle of stall increased with Reynolds number. The maximum C_L defined at the stall angle and showed vary with Reynolds number due to viscous effects, which had 10% bigger values at ReC=1.9x10^5[4].

The computed values of lift coefficient agree well with the experimental results up to the stall angle. At the stall angle, the experimental value of lift coefficient drops abruptly, while the computed lift coefficient continues to increase fig 16. Some of the models did not converge near and above stall angle. Computations done with *k-ε* RNG turbulence model provided converged solutions for angle of attacks near and above stall angle. When compared with clean airfoil at a given angle of attacks of 10°, increase in C_L for 0.5%, 1%, 1.5%, 2%, 3%, and 4% flap height is 25%, 36%, 47%, 53%, 67%, and 77%, respectively. Drastic rise in drag for 3%and 4% flap heights is seen in fig 17.

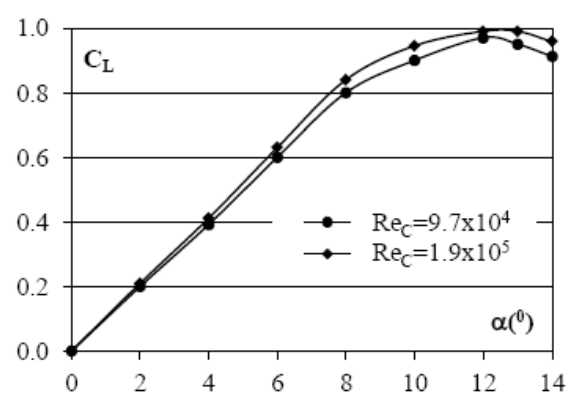

Fig 15- Lift characteristics of airfoil at different Reynolds numbers

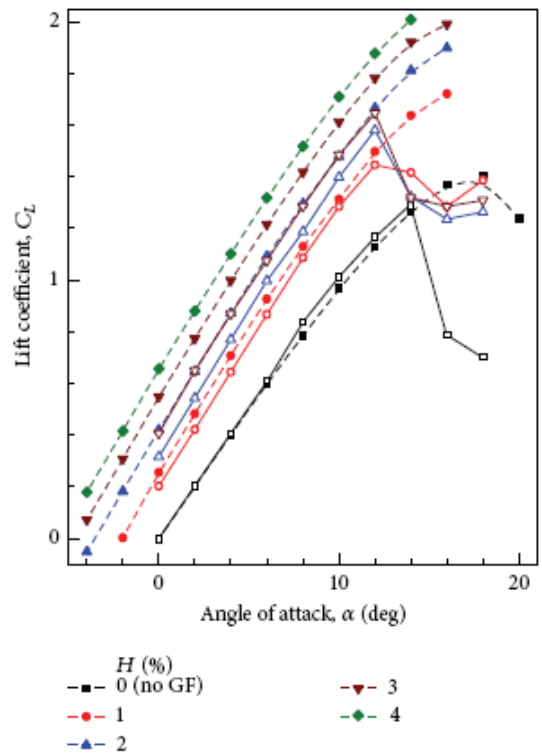

Fig 16- Variation of lift coefficient with angle of attack at different gurney flap heights. Closed symbol + dashed line: Computational results, Open symbol + solid line: Experimental results

For both airfoils without and with gurney flap, the agreement between experimental and computed static pressure distribution is very good even near gurney flap fig 18. Increased suction on suction surface and increased pressure on pressure surface are clearly noticeable on installation of gurney flap, which results in lift enhancement.

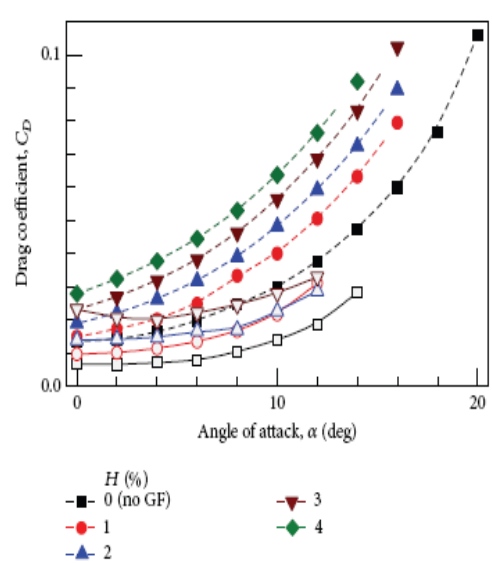

Fig 17- Variation of drag coefficient with angle of attack at different gurney flap heights. Closed symbol + dashed line: Computational results. Open symbol + solid line: Experimental results

Volume : 5 | Issue : 4 | April 2015 | ISSN - 2249-555X

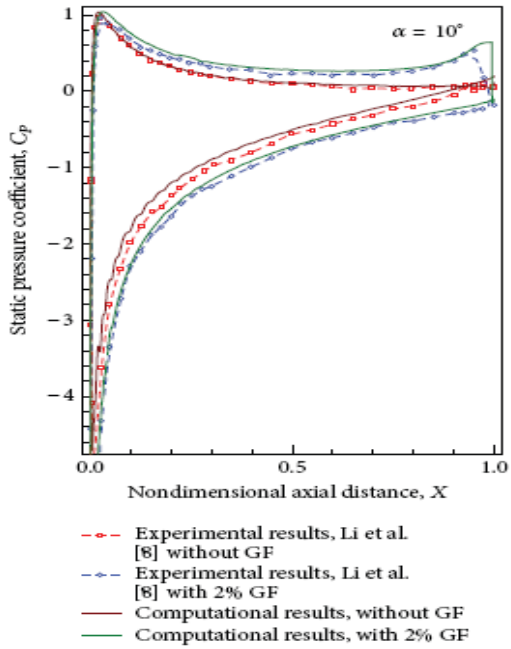

Fig 18- Static pressure distributions for 10^0 angles of attack for 2% gurney flap.

Although suction is increased throughout the surface, the difference is maximum near the trailing edge where the GF is installed. When GF height is increased the maximum suction on the suction surface increases by 27.5%, 39.6%, 50.2%, and 60.3%, respectively, when the GF height is 1%, 2%, 3%, and 4% compared to that on the airfoil without gurney flap fig 19. However the difference in static pressure distribution reduces as the gurney flap height increases [5].

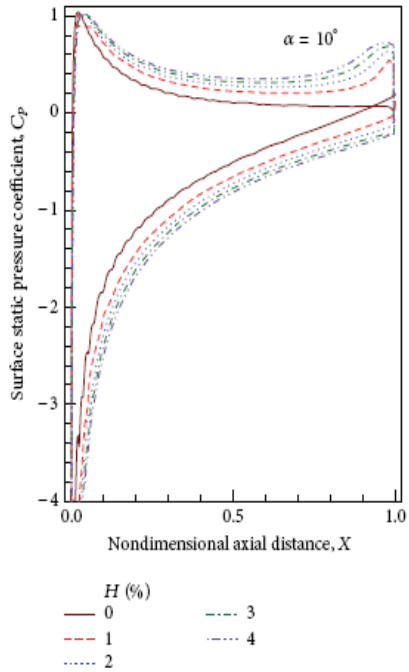

Fig 19- Static pressure distributions for different gurney flap heights at angle of attacks = 10°

CONCLUSIONS

Higher lift at increasing deflected angle limits the speed as higher speed increases drag. The most appropriate turbulence model for middle range Reynolds number & higher angle of attack simulations is the Spalart - Allmaras one-equation model. Otherwise k-□□SST model is best suited for airfoil analysis. Height of 1%*c* has shown better increment in lift-to drag ratio at various angles of attack. Pressure distribution curves show that Gurney flap increases upper surface suction and lower surface high pressure which results in lift enhancement. Pressure coefficient of the suction side of the airfoil initially increased near the leading edge and then showed a monotonously decrease up to trailing edge for all angle of attack. The C_p curves showed similar distributions both Reynolds number. The lift coefficients reached maximum values at stall angle which was 12^0 and 13^0 at Reynolds number =$9.7x10^4$ and $1.9x10^5$, respectively. The angles of stall and lift coefficients increased with Reynolds number. The agreement between computed and experimental values of lift coefficient is very good up to stall angle. Near and above stall angle, the lift coefficient continues to increase. Lift increment decreases for greater heights and drag increases rapidly for$H$ > 2%.

REFERENCE [1] Tousif Ahmed, Md. Tanjin Amin, S.M. Rafiul Islam & Shabbir Ahmed(2013), Computational Study of Flow Around a NACA 0012 Wing Flapped at Different Flap Angles with Varying Mach Numbers, Global Journals Inc. (USA), ISSN: 2249-4596. | [2] Md. Arfan Uddin and A.B.M. Toufique Hasan (2011), A CFD analysis on the effects of geometry of gurney flap on aerodynamics of NACA0012 airfoil, International Conference on Mechanical Engineering, Dhaka. | [3] Eleni C. Douvi, Athanasios I. Tsavalos, Dionissios P. Margaris(2010), CFD calculations of the flow over a NACA0012 airfoil, 4th International Conference from Scientific Computing to Computational Engineering, University of Patras, Dept. of Mechanical Engineering and Aeronautics, Patras, Greece. | [4] Onur Yemenici (2013), Experimental Investigation of the Flow Field around NACA0012 Airfoil, International Journal of Sciences (ISSN 2305-3925). | [5] Shubham Jain, Nekkanti Sitaram, and Sriram Krishnaswamy (2014), Computational Investigations on the Effects of Gurney Flap on Airfoil Aerodynamics, International Scholarly Research Notices, Hindawi Publishing Corporation. |